Association of Triblock Copolymers of Ethylene Oxide and Butylene Oxide in Aqueous Solution. A Study of $B_nE_mB_n$ Copolymers

Yung-Wei Yang, Zhuo Yang, Zu-Kang Zhou,† David Attwood, and Colin Booth*

Manchester Polymer Centre, Departments of Chemistry and Pharmacy, University of Manchester, Manchester M13 9PL, UK

Received August 25, 1995; Revised Manuscript Received October 23, 1995[⊗]

ABSTRACT: Three oxyethylene/oxybutylene triblock copolymers of similar E-block length but different B-block lengths ($B_4E_{40}B_4$, $B_5E_{39}B_5$, and $B_7E_{40}B_7$) were prepared by sequential anionic polymerization and characterized by gel permeation chromatography and NMR spectroscopy. Their association in aqueous solution was investigated by static and dynamic light scattering, and evidence was found for small molecular associates, micelles, and micelle clusters (bridged micelles). Values of the critical micelle concentrations and micellar association numbers were determined and compared with those for related diblock (E_mB_n) and triblock ($E_mB_nE_m$) copolymers.

1. Introduction

Most studies of the micellization of water-soluble block copolymers have been carried out using oxyethylene/oxypropylene triblock copolymers, $E_mP_nE_m$. Here E represents an oxyethylene unit and P an oxypropylene unit. The current state of this work can be judged from recent publications and the references contained therein.[1−7] The effect of block structure on micellization and gelation is of interest, but investigation of this aspect has been held back by lack of suitable samples. A limited range of triblock $P_nE_mP_n$ copolymers are available commercially and have been studied recently.[3,8,9] Diblock E_mP_n copolymers must be specially synthesized and, with one exception,[5] have been largely neglected.

Much of our recent work has been concerned with oxyethylene/oxybutylene block copolymers. A few E_mB_n and $E_mB_nE_m$ copolymers (B represents an oxybutylene unit) are available from Dow Chemical Co.[10,11] However, the samples used in our studies of $E_mB_nE_m$[12−14] and E_mB_n[15−18] copolymers, including comparative studies of oxyethylene/oxybutylene block copolymers with different architectures,[19,20] were all synthesized in our laboratory. As explained previously,[12−20] replacement of propylene oxide by 1,2-butylene oxide carries with it advantages in the polymerization chemistry, as well as providing a block unit of considerably enhanced hydrophobicity.[20] Indeed, this hydrophobicity ensures association in dilute solution even in the case of copolymers with blocks as short as B_4.[17,19]

Several theoretical studies of association of block copolymers have been published in recent times, many of which spring from the related problem of microphase separation in bulk and concentrated solution systems. The topic has been reviewed.[21,22] Most theories are directed toward the simplest problem of diblock copolymers. The general proposition, formulated by ten Brinke and Hadziioannou[23] that the entropy loss associated with looping of the middle block of a symmetrical triblock copolymer affects its micellization is not in doubt, though they overestimated its importance, as shown by a number of more recent theoretical studies.[24−28] Empirically, the effect can be seen in the critical concentrations for micellization of diblock and triblock E/B copolymers of comparable overall chain length and composition: e.g. cmc values of approximately 0.3 and 30 g dm^{-3}, respectively, for copolymers $E_{41}B_8$ and $B_4E_{40}B_4$ in aqueous solution at 40 °C.[19]

The association of triblock copolymers when water is a selective nonsolvent for the outer blocks is particularly interesting. Compared at constant chain length and composition, the effect on the critical concentration for association of changing the structure from an insoluble inner block to insoluble outer blocks can be large: e.g. from 0.9 to 91 g dm^{-3} for copolymers $E_{13}P_{30}E_{13}$ and $P_{14}E_{24}P_{14}$[8] at 40 °C. The effect on association number can also be large, with lower values reported for copolymers with insoluble outer blocks.[8,19] However, micellization of copolymer $P_{21}E_{25}P_{21}$ was not detected either by a dye solubilization method[3] or by measurement of surface tension,[29] and the overall situation is not yet clear.

For solutions of $B_nE_mB_n$ and $P_nE_mP_n$ copolymers in water, micellar association involves copolymer chains either with both end blocks in the core (loops) or with one end block in the core and the other in the fringe. Other possibilities are (i) intermolecular association *via* end blocks and (ii) intermicellar association *via* copolymer chains forming bridges between micelles. Such associations have been predicted[26−28,30,31] and one or more have been identified experimentally for triblock copolymers in aqueous[8,9,19] and organic[25,26,32−34] solvents. For example, copolymer $P_{15}E_{156}P_{15}$, with a lengthy central E block, was shown[9] (by neutron scattering, light scattering, and rheology) to form network structures linked, at high enough concentrations, by micellar associates. In fact, for aqueous micellar systems, linking by chains with end blocks in different micelles is not in doubt. Indeed, if the end blocks are sufficiently hydrophobic then truly elastic networks which are cross-linked by micelles but completely stable to dilution can be formed, e.g. from $C_nE_mC_n$ triblock copolymers with lengthy alkyl blocks.[35,36]

For relatively low-molar-mass copolymers, such as the $B_nE_mB_n$ of present interest, which are favorable to micellization at low to moderate concentrations, the picture which emerges is formation of micelles with the

† EPSRC Visiting Fellow. Permanent address: Department of Chemistry, New York State University at Stony Brook, Stony Brook, NY 11794-3400.

[⊗] Abstract published in *Advance ACS Abstracts,* December 1, 1995.

0024-9297/96/2229-0670$12.00/0

Table 1. Characteristics of the Block Copolymers

precursor block	M_{pk}/g mol^{-1} (GPC[a])	M_w/M_n (GPC[b])	M_n/g mol^{-1} (NMR)	copolymer	M_{pk}/g mol^{-1} (GPC[a])	M_w/M_n (GPC[b])	x_E	M_n/g mol^{-1} (NMR)	M_w/g mol^{-1} (NMR, GPC[c])
E_{40}	1840	1.12	1750	$B_4E_{40}B_4$	2660	1.05	0.83	2340	2460
E_{39}	1650	1.03	1720	$B_5E_{39}B_5$	2340	1.02	0.80	2440	2490
E_{40}	1740	1.04	1760	$B_7E_{40}B_7$	2750	1.03	0.74	2770	2850

[a] Molar mass as if poly(oxyethylene). [b] Corrected for spreading. [c] Calculated from M_n and M_w/M_n of copolymer.

soluble blocks in the fringe and most insoluble blocks in the core, but with a fraction of insoluble blocks extending into the solvent and available for attractive interaction. The present work was undertaken with this framework in mind. Specifically, we undertook a study of a series of copolymers, $B_4E_{40}B_4$, $B_5E_{39}B_5$, and $B_7E_{40}B_7$, of similar overall chain length and composition. The series progresses from weakly (B_4) to strongly (B_7) associating end blocks and so is suited to experimental investigation of predicted effects.[27,30] As mentioned above, a study of one of these copolymers ($B_4E_{40}B_4$) has been reported previously.[19] The small amount of copolymer $B_4E_{40}B_4$ which remained was used to make the limited range of new measurements which are included in this paper.

A related interest, stemming from previous work,[19] lies in the fact that thermally reversible sol → gel → sol transitions were observed on heating or cooling of concentrated solutions of diblock copolymer $E_{41}B_8$, but concentrated solutions of the other triblock copolymers of similar chain length and composition ($E_{21}B_8E_{21}$ and $B_4E_{40}B_4$) did not gel in the temperature range studied. Attention will be paid to this aspect in a subsequent paper.[37]

2. Experimental Section

2.1. Preparation of Copolymers. The copolymers ($B_4E_{40}B_4$, $B_5E_{39}B_5$, and $B_7E_{40}B_7$) were prepared by sequential anionic polymerization of ethylene oxide and 1,2-butylene oxide. All reagents were distilled and dried before use, and vacuum line and ampule techniques were used in order to minimize initiation by moisture at any stage. Initiator solutions were prepared by reacting freshly cut potassium with diethylene glycol, a ratio of [OH]/[OK] ≈ 9 being used to ensure a controlled rate of polymerization. The procedure used was identical to that described previously.[19]

2.2. Characterization of Copolymers. The prepared samples were characterized by gel permeation chromatography (GPC) and nuclear magnetic resonance spectroscopy (NMR). The GPC system consisted of four μ-Styragel columns (Waters Associates, nominal porosities from 500 to 10^6 Å) eluted by tetrahydrofuran (THF) at room temperature and a flow rate of 1 cm^3 min^{-1}. Samples were dissolved in THF at a concentration 2 g dm^{-3}, and their emergence was detected by differential refractometry (Waters Associates Model 410). Calibration was with a series of poly(oxyethylene) samples of known molar mass, and derived molar masses were based on poly(oxyethylene). For ^{13}C NMR spectroscopy, polymer samples were dissolved in $CDCl_3$ (0.1 g cm^{-3}) and spectra were obtained by means of a Varian Unity 500 spectrometer operated at 125.5 MHz. Spectral assignments were taken from previous work.[38]

The GPC curves directly gave values of the molar mass at the peak (M_{pk}), and further analysis gave an estimate of the ratio of mass-average to number-average molar mass (M_w/M_n). The ^{13}C NMR spectra were used primarily to determine number-average molar mass (M_n from integrals of end and chain groups) and average composition (i.e. mole fraction of E, x_E). The molar masses and molecular formulae of the copolymers listed in Table 1 were obtained by combining the number-average molar masses of the precursor blocks and the compositions of the copolymers, both determined by NMR. All end groups of the B blocks were hydroxy groups; i.e. no unsaturated end groups were detected.

2.3. Purification of Copolymers. The purity of the block copolymers was checked by comparing the intensities of resonances from end-group carbons with those from carbons associated with EB block junctions. In each case a small excess of hydroxy end groups over EB junctions was found, although the amount was not outside the experimental error. It was possible that small quantities of homopoly(oxybutylene) had been initiated by introduction of small amounts of moisture with the second monomer. Because of the high reactivity of ethyleneoxy anions compared with butyleneoxy anions,[10] molecules with residual E ends (e.g. diblock copolymers) were statistically very improbable. Accordingly, the copolymers were purified, either by precipitation from dilute solution in dichloromethane or by repeatedly equilibrating them with warm hexane and separating the solid and liquid phases after cooling to 10 °C. Homopoly(oxybutylene) was efficiently removed by either procedure. The presence of even a small proportion of residual poly(oxybutylene) would be expected to lead to insoluble polymer particles in copolymer solutions below the critical micelle concentration. As described below, such particles were not detected in solutions of the purified samples. Within the error of determination, the overall average chain lengths and compositions of the copolymers were unchanged by purification.

2.4. Clouding. Clouding temperatures were determined either by visual observation[19] or by monitoring of the variation of intensity of a laser beam transmitted through the solution and focused on a photodiode detector. The cell containing the solution was immersed in a water bath, the temperature of which was raised slowly (*ca.* 1 K min^{-1}) through the clouding region. Clouding was observed as an abrupt decrease in transmission to a low level. The midpoint of the clouding region was taken as the clouding temperature.

2.5. Static and Dynamic Light Scattering. Solutions for light scattering were clarified by filtering through Millipore Millex filters (0.22 μm porosity) directly into the cleaned scattering cell.

Refractive index increments were determined by means of an Abbé 60/ED precision refractometer (Bellingham and Stanley).

Static light scattering (SLS) intensities were measured by means of a Malvern PCS100 instrument with vertically polarized incident light of wavelength 488 nm supplied by an argon ion laser (Coherent Innova 90) operated at 500 mW or less. The intensity scale was calibrated against benzene. Measurements were made at angles of 45°, 90°, and 135° to the incident beam. In an experiment, measurements were made either on solutions at a given temperature over a range of concentrations, or on solutions of given concentration over a range of temperatures. In the latter case, the temperature of the scattering cell was raised or lowered at *ca.* 1 K min^{-1}.

Dynamic light scattering (DLS) measurements were made by means of the Malvern instrument described above combined with a Brookhaven BI 9000 AT digital correlator. Measurements of scattered light were usually made at an angle of 90° to the incident beam, but some measurements were made at smaller angles (30°, 45°). For micellar solutions (concentration substantially higher than the cmc), the experiment duration was 5−10 min for each correlation function. For predominantly molecular solutions (concentration below or just above the cmc), the experiment duration was increased to 30 min or more in order to increase the precision of the correlation functions. The measurement for each solution was repeated five times.

In designing the light scattering experiments, account was taken of the small size (equivalent hard-sphere radius $r < 20$ nm) expected for the micelles in relation to the value of the scattering vector [$q = (4\pi n/\lambda)\sin(\theta/2)$, n = refractive index of medium, λ = wavelength of light, θ = scattering angle]. Since micelle size depends on the reciprocal of q, the relevant

parameter for assessing intraparticle interference is the dimensionless product qr, and in our experiments qr was generally less than 0.25. The structure factor depends on the volume fraction of swollen particles as well as the mass concentration, and interparticle interference at a given mass concentration can also be quantified in terms of qr. Under our conditions, the light-scattering experiments were effectively carried out at the $qr \rightarrow 0$ limit, and errors in derived quantities (e.g. molar mass, diffusion coefficient, virial coefficients) originating from measurements taken at $\theta = 90°$ (rather than $\theta = 0°$) were significantly less than 1%, i.e. unimportant compared with other sources of error. At all times, experiments made using scattering angles smaller than 90° gave consistent results.

The correlation functions from dynamic light scattering (DLS) were analyzed by the constrained regularized CONTIN method,[39] thus gaining information on the distribution of decay rates (Γ). The distributions so obtained gave distributions of apparent diffusion coefficients ($D_{app} = \Gamma/q^2$) and hence distributions of apparent hydrodynamic radii ($r_{h,app}$, radius of the hydrodynamically equivalent hard sphere corresponding to D_{app}) *via* the Stokes−Einstein equation

$$r_{h,app} = kT/(6\pi\eta D_{app}) \quad (1)$$

where k is the Boltzmann constant and η is the viscosity of water at temperature T. Values of η were taken from ref 40.

The basis for analysis of static light scattering (SLS) was the Rayleigh−Gans−Debye equation, used here in the form

$$I - I_s = K^* c M_w \quad (2)$$

where I is intensity of light scattered from solution relative to that from benzene, I_s is the corresponding quantity for pure solvent, c is the concentration (in g dm^{-3}), M_w is the mass-average molar mass of the solute, and

$$K^* = (4\pi^2/N_A\lambda^4)(n_B^2/R_B)(dn/dc)^2$$

where N_A = Avogadro's constant, n_B and R_B = the refractive index and Rayleigh ratio of benzene, respectively, and dn/dc = the refractive index increment. The value of the refractive index increment for the present copolymers in water was 0.133 ± 0.002 cm^3 g^{-1} at 30 °C, i.e. within experimental error the same as that obtained previously[15,17,20] for aqueous solutions of comparable samples. The temperature derivative of dn/dc obtained previously[15] (i.e. -2×10^{-4} cm^3 g^{-1} K^{-1}) was used to derive values of K^* for the other temperatures considered. Values of the refractive index of benzene were taken from refs 41 and 42

$$n_B = 1.51313[1 - 64 \times 10^{-5}(T - 20)] \quad (488 \text{ nm}, T \text{ in °C})$$

and those of the Rayleigh ratio of benzene were from ref 43

$$(R_B/\text{cm}^{-1}) = 3.20 \times 10^{-5}[1 + 0.368 \times 10^{-2}(T - 25)] \quad (488 \text{ nm}, T \text{ in °C})$$

3. Results and Discussion

3.1. Clouding. The clouding temperatures of 2 wt % solutions of copolymers $B_4E_{40}B_4$, $B_5E_{39}B_5$, and $B_7E_{40}B_7$ were 61.0, 42.8, and 25.7 °C, respectively. As described below, light-scattering measurements were made on solutions at temperatures within 3−6 °C of their cloud points. Under these conditions, the turbidities of selected solutions were monitored at intervals over a period of days and were found to be stable. In this respect, we note that investigations of micellar solutions of related surfactants have been shown to give valid results up to the clouding temperature.[44]

3.2. Intensity Distributions of Hydrodynamic Radius. DLS measurements on solutions of copolymer $B_7E_{40}B_7$ were carried out at 20 °C. Selected intensity-fraction distributions of log $r_{h,app}$ are illustrated in Figure 1. The distributions obtained for solutions in the concentration range 5−40 g dm^{-3} contained two peaks, one attributed to micelles ($r_{h,app} = 7-9$ nm) and a second attributed to molecules ($r_{h,app} \approx 1-2$ nm); see Figure 1. At higher concentrations (range 60−100 g dm^{-3}), the distribution was resolved into three components, attributed to unassociated molecules ($r_{h,app} \approx 1-2$ nm), molecular (as distinct from micellar) associates ($r_{h,app} \approx 3-5$ nm), and micelles (10−20 nm); see, for example, Figure 1. The intensities of the peaks were dependent on the concentrations and molar masses of the various species, as discussed in detail in section 3.6. At low concentrations (e.g. $c = 2$ g dm^{-3}) a single broad peak was obtained. Several attempts, using different scattering angles, were made to resolve two peaks for this dilute solution, but without success. The effect was judged to be a consequence of the constraints of the CONTIN method when applied to systems of low scattering intensity, i.e. to the precision of our data defining the correlation function being too low to permit an acceptable "two-peak" solution. It was possible to force a fit to a two-exponential function (or an exponential plus stretched exponential function[26]), but we preferred to accept the discipline of the CONTIN method.

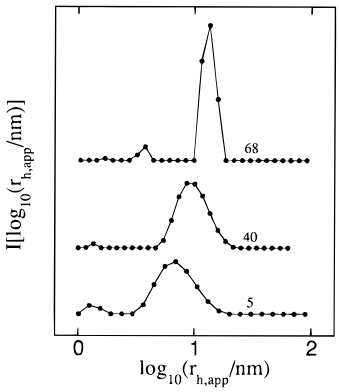

Figure 1. Dynamic light scattering from aqueous solutions of copolymer $B_7E_{40}B_7$ at 20 °C and concentrations 5, 40, and 68 g dm^{-3} (as indicated). The plots are of intensity fraction of logarithmic apparent hydrodynamic radius, i.e. $I(\log r_{h,app})$ *versus* $\log r_{h,app}$.

Examples of intensity-fraction distributions of log $r_{h,app}$ obtained for solutions of copolymer $B_5E_{39}B_5$ at 40 °C are shown in Figure 2. At high concentrations ($c >$ 50 g dm^{-3}) the distributions contained two peaks, attributed to molecules ($r_{h,app} = 2-3$ nm) and micelles ($r_{h,app} = 9-14$ nm); see Figure 2a. At low concentrations ($c \leq 40$ g dm^{-3}) the distributions contained single broad peaks which overlapped the size ranges of those obtained at higher concentrations; see Figure 2a. A broad peak is explained by the CONTIN program rejecting a "two-peak" solution (molecules and micelles) in favor of a more conservative "broad peak" solution, as would be expected if the data points defining the correlation function were insufficiently precise. The effect of temperature was explored for a single high concentration (120 g dm^{-3}, see Figure 2b). This restriction was imposed in order to maximize the precision of the data. As expected, the intensity fraction of micelles increased as temperature was increased. The effect of temperature on the apparent hydrodynamic radius of the micelles was small, which was consistent with results for many other E/B and E/P block copolymer micelles. This effect was explained many years ago[45] as a decrease in swelling of the E-block fringe in the poorer solvent at higher temperature compensating an increase in association number. The pronounced effect of tem-

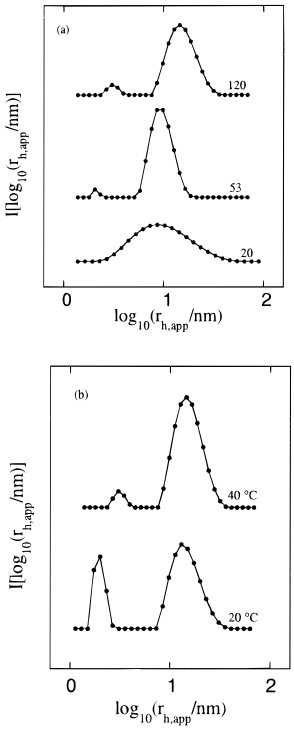

Figure 2. Dynamic light scattering from aqueous solutions of copolymer $B_5E_{39}B_5$: (a) at 40 °C and concentrations 20, 53, and 120 g dm^{-3} (as indicated); (b) of concentration 120 g dm^{-3} at temperatures 20 and 40 °C (as indicated). The plots are of intensity fraction of logarithmic apparent hydrodynamic radius, i.e. $I(\log r_{h,app})$ *versus* $\log r_{h,app}$.

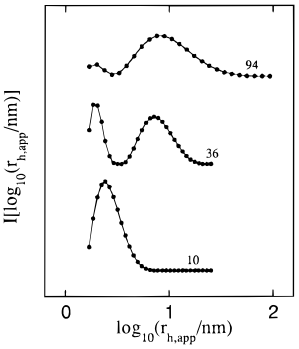

Figure 3. Dynamic light scattering from aqueous solutions of copolymer $B_4E_{40}B_4$ at 50 °C and concentrations 10, 36, and 94 g dm^{-3} (as indicated). The plots are of intensity fraction of logarithmic apparent hydrodynamic radius, i.e. $I(\log r_{h,app})$ *versus* $\log r_{h,app}$.

perature and concentration on the apparent hydrodynamic radius of the molecules is discussed in section 3.4.

An intensity distribution of $\log r_{h,app}$ for a 60 g dm^{-3} solution of copolymer $B_4E_{40}B_4$ at 50 °C has been published.[19] That distribution was single-peaked and broad. The new measurements, made with improved equipment, achieved better resolution, with distributions of the form shown in Figure 3. For solutions at 50 °C and concentrations in the range 30−120 g dm^{-3}, the intensity distributions of $\log r_{h,app}$ contained two peaks, attributed to micelles ($r_{h,app}$ = 7−8 nm) and molecules ($r_{h,app} \approx 2$ nm). At $c = 10$ g dm^{-3} the intensity distribution contained a single peak attributed to molecules.

The accumulated evidence from DLS for the three copolymers is that in each case, under suitable conditions, micelles were formed having narrow logarithmic intensity distributions peaking at $r_{h,app}$ in the range

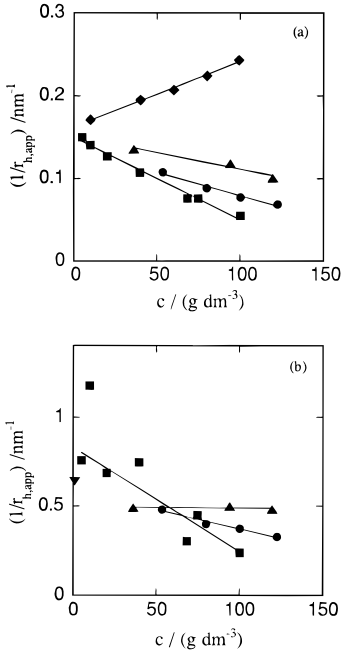

Figure 4. Dynamic light scattering from aqueous solutions of triblock copolymers. Inverse apparent hydrodynamic radius of (a) micelles and (b) molecules *versus* concentration for (◆) $E_{21}B_{11}E_{21}$, 40 °C; (■) $B_7E_{40}B_7$, 20 °C; (●) $B_5E_{39}B_5$, 40 °C; (▲) $B_4E_{40}B_4$, 50 °C; (▼) PEG2000, 25 °C.

7−20 nm. Under all conditions investigated, the micelles were in equilibrium with molecules. It is concluded that micellization of the copolymers occurred by a closed association process. The critical conditions (concentration and temperature) for this micellization are discussed in section 3.5.

3.3. Average Hydrodynamic Radii of Micelles. Intensity-average values of $1/r_{h,app}$ were calculated for micelles by integrating over the micelles peak in the intensity distributions of decay rate. Since the dissymmetry ratio was found to be near to unity, the values obtained were essentially *z*-averages. Unlike the behavior reported for micellar solutions of E_mB_n diblock and $E_mB_nE_m$ triblock copolymers,[15,17−20] the average values of $r_{h,app}$ increased as concentration was increased, i.e. the apparent diffusion coefficient ($D_{app} = kT/6\pi\eta r_{h,app}$) decreased. This effect is shown in Figure 4a, where the intensity average inverse hydrodynamic radii found for micelles of the three $B_nE_mB_n$ copolymers are plotted against concentration and compared with corresponding results for micelles of copolymer $E_{21}B_{11}E_{21}$. The results for copolymer $E_{21}B_{11}E_{21}$ (which is comparable in overall chain length and composition to the $B_nE_mB_n$ copolymers) were taken from ref 20. Plotting $1/r_{h,app}$ rather than D_{app} compensates for any differences in solution temperature and solvent viscosity. The experimental points for the three $B_nE_mB_n$ copolymers lay on straight lines, thus allowing determination of the intensity-average (*z*-average) values of $r_{h,o}$ and D_o (at zero concentration), as listed in Table 2. Within the experimental error (estimated to be ±10%) the values of $r_{h,o}$ were identical. The negative slopes of the plots were in the order $B_7E_{40}B_7 > B_5E_{39}B_5 > B_4E_{40}B_4$.

The concentration dependence of apparent diffusion coefficient (in dilute solution) can be expressed as

$$D_{app} = D_o(1 + k_d c) \qquad (3)$$

where the expansion is truncated at the second term. Parameter k_d is related to the thermodynamic second virial coefficient, A_2, through the equation[46]

Table 2. Diffusion Coefficients, Hydrodynamic Radii, and Mass-Average Molar Masses of Micelles of $B_nE_mB_n$ Copolymers in Aqueous Solution[a]

copolymer	T/°C	$10^{11}D_o$/ $m^2\ s^{-1}$	$r_{h,o}$/ nm	$10^{-4}M_w$/ $g\ mol^{-1}$	N_w
$B_4E_{40}B_4$	50	6.6	6.6	2.7 ± 1.0	11
$B_5E_{39}B_5$	40	4.8	7.4	4.7 ± 1.0	19
$B_7E_{40}B_7$	20	3.2	6.7	5.0 ± 0.5	18

[a] Values of $(D_o)_z$ and $(1/r_{ho})_z^{-1}$ obtained by extrapolation to zero concentration (Figure 4a). Estimated error in D_o and r_{ho}, ±10%; in M_w and N_w, ±20%.

$$k_d = 2A_2M_w - k_f - 2v \qquad (4)$$

where M_w is the mass-average molar mass, k_f is the frictional coefficient, and v is the partial specific volume of the micelles in solution. If the quantities M_w, k_f, and v are independent of concentration, the sign of k_d depends on the sign and size of A_2, which in turn depends on the nature of the intermicellar interaction, i.e. on the micellar excluded volume. The nature of the present results, i.e. the negative slopes of the plots of $1/r_{h,app}$ *versus* c found for the $B_nE_mB_n$ copolymer micelles compared with the positive slope found for $E_mB_nE_m$ copolymer micelles (see Figure 4a), implies a substantial attractive contribution to their intermicellar interaction, resulting in small excluded volumes for the micelles of the $B_nE_mB_n$ copolymers, which in turn results in small values of A_2 and so negative values of k_d (*via* eq 4). This is consistent with the micelles having a fraction of their B-blocks extended into the solvent and available for interaction, either with B-blocks from chains originating from a second micelle[34] or by entering the core of a second micelle.[27,30] In either case, the effect results in transient micellar linking, which implies a second equilibrium in the system:

$$NA \rightleftarrows A_N \qquad \text{(molecule/micelle equilibrium)}$$

$$MA_N \rightleftarrows (A_N)_M \qquad \text{(micelle/linked-micelles equilibrium)}$$

The increase in negative slope of $1/r_{h,app}$ *versus* c with an increase in B-block length (see Figure 4a) is consistent with a larger attractive contribution associated with a longer B-block.

3.4. Average Hydrodynamic Radii of Molecules and Molecular Associates. Intensity-average (z-average) values of $1/r_{h,app}$ were calculated for molecules plus molecular associates by integrating over the relevant peaks in the intensity distributions of decay rate. The values of $(1/r_{h,app})_z$ so obtained were scattered, particularly so when the intensity fractions were small; see Figure 4b. A dilute solution of nonassociating polymer of similar chain length (polyethylene glycol PEG2000, E_{45}) was included in the experiments and gave consistent results. Generally, $1/r_{h,app}$ was reduced as concentration was increased, the exception being copolymer $B_4E_{40}B_4$ in solution at 50 °C, for which $1/r_{h,app}$ was independent of concentration. The concentration dependences (negative slopes) were in the order $B_7E_{40}B_7 \gg B_5E_{39}B_5 > B_4E_{40}B_4$.

For copolymers $B_7E_{40}B_7$ and $B_5E_{39}B_5$, the effect of concentration lends support to the view[25,27,30] that for molecules of this type limited open molecular association accompanies closed association to micelles. This means (in a simplified model) that four components are in equilibrium: molecules, molecular associates (linked molecules), micelles, and micellar associates (linked micelles)

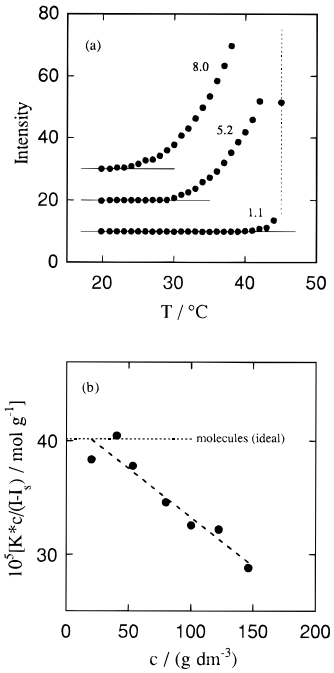

Figure 5. Determination of cmc and cmt for aqueous solutions of copolymer $B_5E_{39}B_5$. (a) Intensity of light scattered from solution *versus* temperature for solutions with the concentrations (g dm^{-3}) indicated. The full lines represent scattering from solutions of unassociated copolymer molecules. The dotted line represents the cloud point of dilute solution. For clarity, the curves are arbitrarily shifted on the ordinate. (b) Debye plot for solutions at 20 °C. The dashed line is the least squares fit through the points above the cmc. The dotted line represents the Debye function for ideal solutions of copolymer molecules. See section 2.5 for definition of K^*, I, and I_s.

$$LA \rightleftarrows A_L \qquad \text{(molecules/linked molecules)}$$

$$NA \rightleftarrows A_N \qquad \text{(molecules/micelles)}$$

$$MA_N \rightleftarrows (A_N)_M \qquad \text{(micelles/linked micelles)}$$

The ordinate intercepts in Figure 4b gave similar values of $r_{h,o}$ for copolymers $B_4E_{40}B_4$ and $B_5E_{39}B_5$ (2.0 ± 0.1 and 1.7 ± 0.1 nm respectively) but a smaller value for copolymer $B_7E_{40}B_7$ ($r_{h,o} = 1.2 \pm 0.2$ nm). The smaller value found for molecules of copolymer $B_7E_{40}B_7$ may arise from intramolecular association of the B_7 blocks.

3.5. Critical Micelle Concentrations and Temperatures. Critical micelle temperatures (cmt) for solutions of copolymer $B_5E_{39}B_5$ were determined as the temperature at which static light scattering intensity from a heated solution of given concentration departed significantly from a baseline value established for molecules; see Figure 5a. For the same system, the critical micelle concentration (cmc) at 20 °C was determined as the lowest concentration at which the Debye function for a series of solutions at given temperature departed significantly from a value characteristic of molecules; see Figure 5b. The cmt and cmc values of solutions of copolymer $B_7E_{40}B_7$ were too low to allow their determination by the methods described above. In this case the excess intensity $I - I_s$ plotted against concentration was found to be linear up to $c = 40$ g dm^{-3}, and extrapolation to the value expected for a molecular solution could be used to obtain a value of the cmc; see Figure 6. The linear relationship was probably a consequence of the attractive contribution to the micellar interaction (described in section 3.3) moderating the effect of hard-sphere repulsion, to give

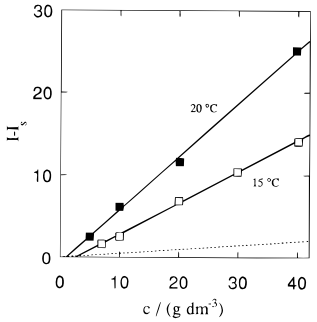

Figure 6. Static light scattering function ($I - I_s$) *vs* c for aqueous solutions of $B_7E_{40}B_7$ at (■) 20 °C and (□) 15 °C. The full lines are least-squares fits. The dashed line represents scattering from solutions of unassociated copolymer molecules.

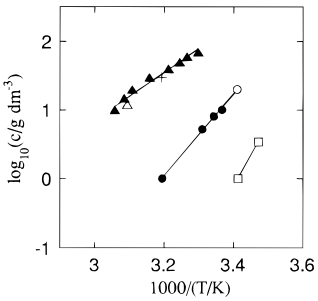

Figure 7. Critical conditions for micellization. Logarithm of copolymer concentration versus inverse temperature for solutions of copolymers (□) $B_7E_{40}B_7$, (●, ○) $B_5E_{39}B_5$ and (▲, △, +) $B_4E_{40}B_4$. Filled symbols indicate results obtained by the cmt method. Unfilled symbols indicate results obtained by the cmc methods; see the text. (+) indicates a result obtained by measurement of surface tension. The results for copolymer $B_4E_{40}B_4$ obtained by the cmt and surface tension methods were taken from ref 19.

Table 3. Critical Micelle Temperatures and Concentrations for Solutions of $B_nE_mB_n$ Copolymers

copolymer	method	T/°C	c/g dm^{-3}	ref
$B_7E_{40}B_7$	SLS−cmc	20	1.0	present work
		15	3.4	
$B_5E_{39}B_5$	SLS−cmc	20	20	present work
$B_5E_{39}B_5$	SLS−cmt	24	10	present work
		26	8.0	
		29	5.2	
		40	1.1	
$B_4E_{40}B_4$	γ−cmc	40	30	19
$B_4E_{40}B_4$	SLS−cmc	50	12	present work
$B_4E_{40}B_4$	SLS−cmt	54	10	19
		51	15	
		48.5	20	
		43.5	30	
		38	40	
		35	50	
		33	60	
		30	70	

an approximately ideal solution over the low concentration range. This effect is described further in section 3.6. The values of the cmc obtained in this way for aqueous solutions of copolymer $B_7E_{40}B_7$ were 1.0 g dm^{-3} at 20 °C and 3.4 g dm^{-3} at 15 °C.

Values of the cmc obtained for copolymer $B_5E_{39}B_5$ and $B_7E_{40}B_7$, and those obtained previously[19] for copolymer $B_4E_{40}B_4$, are listed in Table 3 and plotted as log c *versus* $1/T$ in Figure 7. For purposes of comparison, the best straight lines drawn through the data points were used (by interpolation or extrapolation as necessary) to obtain approximate values of the cmc at a common temperature of 20 °C (3.41 on the abscissa of Figure 7) for the three copolymers: i.e., $B_4E_{40}B_4$, 190 g dm^{-3}; $B_5E_{39}B_5$, 20 g dm^{-3}; $B_7E_{40}B_7$, 1.0 g dm^{-3}.

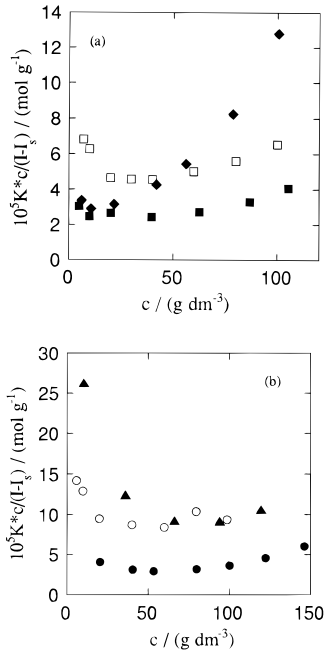

Figure 8. Debye plots for aqueous solutions of triblock copolymers: (a) $B_7E_{40}B_7$ at (■) 20 °C and (□) 15 °C; (◆) $E_{21}B_{11}E_{21}$ at 20 °C; (b) $B_5E_{39}B_5$ at (●) 40 °C and (○) 30 °C; (▲) $B_4E_{40}B_4$ at 50 °C. See section 2.5 for definition of K^*, I, and I_s.

3.6. Molar Masses from Static Light Scattering. Debye plots for solutions of copolymer $B_7E_{40}B_7$ at 15 and 20 °C and over a wide concentration range are shown in Figure 8a. The plots indicate associates of higher molar mass at 20 °C compared with 15 °C, as expected for the poorer solvent at the higher temperature. A corresponding plot for solutions of triblock copolymer $E_{21}B_{11}E_{21}$ at 20 °C (see Figure 8a) provides a useful comparison, since the plots have similar values of the Debye function at $c \rightarrow 0$, indicative of similar micellar molar masses. (The data for copolymer $E_{21}B_{11}E_{21}$ come from ref 20.) The overall scattering behavior of copolymer $B_7E_{40}B_7$ solutions is consistent with closed association into micelles, but the slopes and curvatures of the Debye plots at high concentration are much changed compared with that shown for copolymer $E_{21}B_{11}E_{21}$. A low slope is consistent with an attractive contribution to the interaction of $B_7E_{40}B_7$ micelles which is absent in the interaction of $E_{21}B_{11}E_{21}$ micelles, and which is in agreement with our interpretation of the DLS results presented in section 3.2.

Debye curves obtained for copolymer $B_5E_{39}B_5$ at 30 and 40 °C and, in the present work, for copolymer $B_4E_{40}B_4$ at 50 °C, are shown in Figure 8b. A corresponding plot for solutions of copolymer $B_5E_{39}B_5$ at 20 °C, shown in Figure 5b, indicates very limited micellization at that temperature. Other Debye plots for copolymer $B_4E_{40}B_4$ have been published previously[19]. The overall pattern of the results is similar to that illustrated in Figure 8a for solutions of copolymer $B_7E_{40}B_7$. The major difference is the extent of association; i.e. as judged by the overall level of the Debye function, the micellar molar masses rank in the order $B_7E_{40}B_7 > B_5E_{39}B_5 > B_4E_{40}B_4$.

The upturns in the Debye plots at low concentrations are caused by the micelle−molecule equilibrium, i.e. the dissociation of micelles at concentrations approaching the cmc. An approach often used to obtain M_w for the micelles in a system with a non-negligible value of the cmc is to use a Debye plot of $K^*c'/(I - I_s)$ against c', where c' is the copolymer concentration corrected for the concentration of molecules, i.e. c − cmc. The assump-

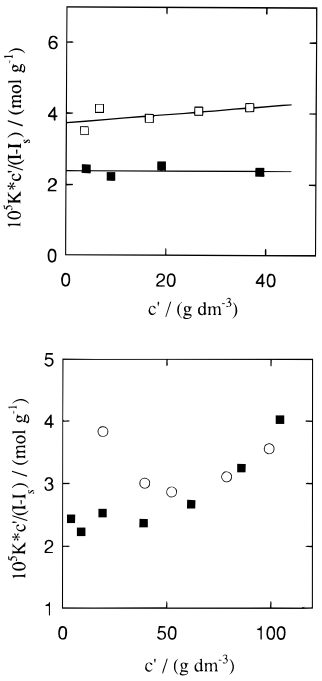

Figure 9. Debye plots corrected using the cmc: (a) aqueous solutions of copolymer $B_7E_{40}B_7$ at (■) 20 °C and (□) 15 °C; (b) aqueous solutions of copolymer $B_7E_{40}B_7$ at (■) 20 °C and (○) copolymer $B_5E_{39}B_5$ at 40 °C. Note that $c' = c -$ cmc. The full lines are the least-squares fits to the points. See section 2.5 for the definition of K^*, I, and I_s.

tions are (i) that the concentration of molecules is equal to the cmc when $c >$ cmc and (ii) that the intensity of scattering from micelles is unchanged by the presence of molecules. This approach was found to be useful for dilute solutions of copolymer $B_7E_{40}B_7$, but not for those of the other two copolymers.

3.6.1. Debye Plots Corrected Using the cmc. Corrected Debye plots for dilute solutions ($c' <$ 40 g dm^{-3}) of copolymer $B_7E_{40}B_7$ are shown in Figure 9a. Linear extrapolations to $c' = 0$ yielded values of mass-average molar masses of $M_w = 42\,000$ and 27 000 g mol^{-1} at 20 and 15 °C, respectively, both to ±5000 g mol^{-1}. Since correction *via* the cmc accounts only for molecules, these values are averages over the other two species in dilute solution, i.e. micelles and molecular associates.

The same method was applied to solutions of copolymer $B_5E_{39}B_5$ at 40 °C (see Figure 9b) but was not successful, as the corrected Debye plot showed significant curvature with an upturn at low concentrations. As seen in Figure 9b, which covers a wide concentration range, the high concentration behavior of both systems ($B_7E_{40}B_7$ at 20 °C, $B_5E_{39}B_5$ at 40 °C) are very similar. The almost ideal behavior of the $B_7E_{40}B_7$ system at low c is attributed to compensating attractive and repulsive interactions of micelles in the dilute solution range, as discussed in section 3.5. The behavior of the $B_5E_{39}B_5$ system reflects more closely the complexity of the present systems.

3.6.2. Debye Plots Corrected Using the Results of Dynamic Light Scattering. In order to deal systematically with solutions of all three copolymers, an alternative approach was adopted, based on that used recently by Lairez *et al.*[26] in their analysis of light scattering from a polystyrene/polyisoprene/polystyrene block copolymer in a selective nonsolvent for polystyrene.

3.6.2.1. Copolymer $B_7E_{40}B_7$. Useful DLS results were obtained for solutions of copolymer $B_7E_{40}B_7$ only at 20 °C. Intensity fractions attributable to molecules (z_m) were obtained as area fractions from the intensity distributions of log $r_{h,app}$; see Table 4. The error in assessing the areas of small peaks was large, particularly since the number of data points defining the peaks was generally no more than four or five. The consequent scatter of results is seen in Figure 10a, where z_m is plotted against copolymer concentration. With an increase in concentration, as micelles were formed, the value of z_m fell rapidly from unity (no micelles) to a minimum value and then increased, as indicated by the dashed curve. The increase is attributable to formation of molecular associates, and the consequent increase in scattering intensity.

Table 4. Intensity and Apparent Mass Fractions of Molecules in Solutions of $B_nE_mB_n$ Copolymers

copolymer	c/g dm^{-3}	T/°C	z_m	$I - I_s$	$c_{m,app}$/g dm^{-3} uncorrected	$c_{m,app}$/g dm^{-3} smoothed
$B_7E_{40}B_7$	100	20	0.078	36	66	66
	75		0.032	36	27	40
	68		0.066	38	53	34
	40		0.012	25	7	14
	20		0.024	12	6	6
	10		0.019	6.2	2.6	3
	5		0.058	2.5	3.0	2
$B_5E_{39}B_5$	123	40	0.056	35	60	58
	100		0.033	37	37	43
	80		0.034	33	34	30
	53		0.024	24	18	18
	123	20	0.26	5.5	40	–
		30	0.15	15	63	–
		40	0.056	35	60	–
$B_4E_{40}B_4$	120	50	0.098	15	49	49
	94		0.085	13	39	40
	66		(0.1)[a]	9.4	32	32
	36		0.35	3.8	45[b]	23

[a] Value estimated from Figure 12a. [b] Value ignored in subsequent analysis.

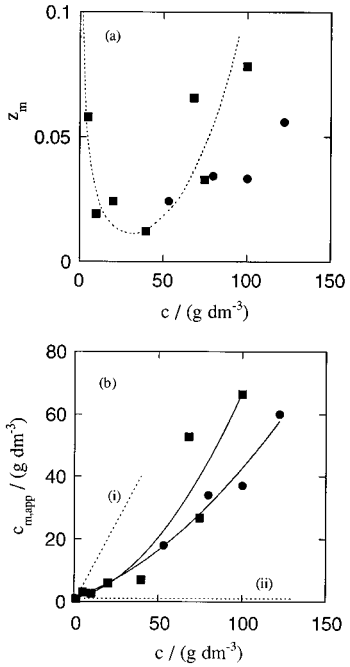

Figure 10. Light scattering from aqueous solutions of copolymers (■) $B_7E_{40}B_7$ at 20 °C and (●) $B_5E_{39}B_5$ at 40 °C: (a) intensity fraction (z_m) attributable to molecules *versus* overall copolymer concentration (c). The dashed curve is intended to lead the eye through the data points for copolymer $B_7E_{40}B_7$ and has no theoretical significance. (b) Apparent concentration of molecules ($c_{m,app}$) *versus* overall copolymer concentration (c). The solid curves were used to smooth the data. The dotted lines are (i) $c_{m,app} = c$ and (ii) $c_{m,app} =$ cmc.

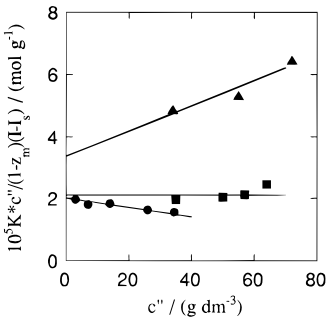

Figure 11. Debye plots corrected using $c_{m,app}$. Results for aqueous solutions of (■) $B_7E_{40}B_7$ at 20 °C, (●) $B_5E_{39}B_5$ at 40 °C, and (▲) $B_4E_{40}B_4$ at 50 °C. Note that $c'' = c - c_{m,app}$, where $c_{m,app}$ is the apparent concentration of molecules and that z_m is the intensity fraction of scattered light attributable to molecules as distinct from micelles. The full lines are least-squares fits to the points. See section 2.5 for the definition of K^*, I, and I_s.

To calculate an average molar mass, it is necessary to know the mass concentration of micelles and intensity associated with the micelles over a range of concentration. The fraction of intensity of scattering associated with micelles is readily obtained as $(1 - z_m)$, but the mass concentration is a problem. If the scattering from molecules were ideal, then at a given copolymer concentration, the contribution from molecules to the excess scattering intensity relative to benzene $(I - I_s)$ could be obtained from

$$z_m(I - I_s) = K^*c_mM_m \qquad (10)$$

where M_m is the known mass-average molar mass of the molecules, and c_m is their mass concentration. However molecular association will enhance the intensity of scattering from the molecules component (by virtue of an increase in average molar mass) compared with the nonassociated case. Moreover, molecular association will increase the equilibrium concentration of molecules (as distinct from micelles), since associated molecules will not be available for closed micellization. The actual concentration and molar mass of the molecules (i.e. combined unassociated and associated forms) cannot be obtained from our experiments, but apparent values of the concentration of molecules ($c_{m,app}$) are available *via* eq 10 (see Table 4 for values) and can be used in the determination of micellar molar mass.

The extent to which the molecules in a solution of copolymer $B_7E_{40}B_7$ depart from their ideal unassociated state can be judged from the plot of $c_{m,app}$ against overall concentration (c) shown in Figure 10b. The values extrapolate to meet the line $c_{m,app} = c$ (labeled i in Figure 10b) at $c \approx 1$ g dm^3, which is in satisfactory agreement with the value estimated for the cmc as described in section 3.5. The departure of the system from the simple closed association model, i.e. $c_{m,app} =$ cmc at all concentrations (represented by line ii in Figure 10b) is seen to be large at high concentrations. Similar behavior was reported by Lairez *et al.*[26]

A corrected Debye plot, i.e. $K^*c''/(1 - z_m)(I - I_s)$ *versus* c'' where $c'' = c - c_{m,app}$, was constructed; see Figure 11. This corrected plot can be compared with the uncorrected plot shown in Figure 8a. In constructing the corrected plot, smoothed values of c'' were taken from the curve shown in Figure 10b. The slope of the Debye plot corrected in this way has no simple interpretation, but the ordinate intercept, which pertains to the infinitely dilute (ideal) micellar state, can be used to calculate the mass-average molar mass of $B_7E_{40}B_7$ micelles in aqueous solution at 20 °C: i.e. $M_w = 50\,000 \pm 5000$ g mol^{-1}. This value is about 20% higher than that obtained using a Debye plot corrected for the cmc (i.e. from Figure 9a), which is reasonable, since the present value is for micelles alone whereas that obtained from Figure 9a was for micelles plus molecular associates. This close correspondence between the two methods when applied to copolymer $B_7E_{40}B_7$ provided justification for the use of the second approach to analyze the more complex cases of the other two copolymers.

3.6.2.2. Copolymer $B_5E_{39}B_5$. Useful DLS results were obtained for solutions of copolymer $B_5E_{39}B_5$ at 40 °C. They were less satisfactory than those obtained for copolymer $B_7E_{40}B_7$, since it proved impossible to resolve molecules and micelles peaks in the intensity distributions for solutions of overall copolymer concentration $c < 50$ g dm^{-3}; see section 3.2. The quantities required for correcting the Debye plot (z_m, $c_{m,app}$) are listed in Table 4 and plotted in Figure 10a,b. In spite of the limited concentration range of the data for copolymer $B_5E_{39}B_5$, the similar consequences of molecular association in the two systems ($B_5E_{39}B_5$ and $B_7E_{40}B_7$) are apparent. Indeed, the results for solutions of copolymer $B_5E_{39}B_5$ at 40 °C almost map onto those for copolymer $B_7E_{40}B_7$ at 20 °C, which is consistent with the two systems being at similar undercoolings with respect to their clouding temperatures; see section 3.1.

The corrected Debye plot for solutions of copolymer $B_5E_{39}B_5$ at 40 °C (constructed using smoothed values of c'') is included in Figure 11. This plot can be compared with the uncorrected plot shown in Figure 9b. The data do not allow close definition of the ordinate intercept, but (*via* the line shown in Figure 11) they are consistent with a value of $M_w = 47\,000 \pm 10\,000$ g mol^{-1}.

3.6.2.3. Copolymer $B_4E_{40}B_4$. Intensity distributions of log $r_{h,app}$ obtained for solutions of copolymer $B_4E_{40}B_4$ at 50 °C showed significant micellization only at concentrations above 35 g dm^{-3}. For all distributions obtained, the molecules' peaks were incompletely defined (see Figure 3), making correction of the Debye plot less certain than for the other systems. Approximate values of z_m and $c_{m,app}$ are listed in Table 4 and plotted against concentration in Figure 12a,b. In Figure 12b an additional point was available from the known[19] cmc of copolymer $B_4E_{40}B_4$, i.e. 16 ± 5 g dm^{-3} at 50 °C. The obviously inaccurate data point at $c = 36$ g dm^{-3} was weighted out of subsequent calculations. In Figure 12b, comparison can be made with the behavior expected for an ideal closed association ($c_{m,app} =$ cmc, line ii) and with that found for copolymer $B_7E_{40}B_7$.

The corrected Debye plot is included in Figure 11, and can be compared with the uncorrected plot shown in Figure 8b. The ordinate intercept of the best straight line through the corrected data leads to a molar mass for $B_4E_{40}B_4$ micelles in aqueous solution at 50 °C of $M_w = 27\,000 \pm 10\,000$ g mol^{-1}.

As seen in Figure 11, the slopes of the corrected Debye plots rank in the order $B_4E_{40}B_4 > B_5E_{39}B_5 > B_7E_{40}B_7$. The trend is consistent with (at most) weak association of the $B_4E_{40}B_4$ micelles and strong association of the $B_7E_{40}B_7$ micelles. In turn, this is consistent with the better solubility of the copolymer with the short B-blocks, the effect of which is also seen in the clouding behaviors of the copolymers: see section 3.1.

3.7. Micellar Associates. As described in section 3.3 and 3.6, the presence of micellar associates was inferred from the concentration dependences of the intensity-averaged hydrodynamic radii and from the slopes of the uncorrected and corrected Debye plots. Direct evidence of micellar association *via* resolution of

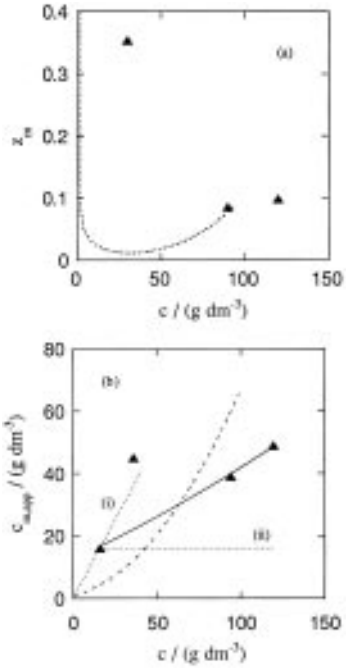

Figure 12. Light scattering from aqueous solutions of copolymer $B_4E_{40}B_4$ at 50 °C. (a) Intensity fraction (z_m) attributable to molecules *versus* overall copolymer concentration (c). (b) Apparent concentration of molecules ($c_{m.app}$) *versus* overall copolymer concentration (c). The solid line was used to smooth the data, the point at $c = 36$ g dm^{-3} being ignored. The dotted lines represent (i) $c_{m,app} = c$ and (ii) $c_{m,app} =$ cmc. In both a and b the dashed curves represent the results for copolymer $B_7E_{40}B_7$ (see Figure 10b) and are included for comparison.

a peak at high values of log $r_{h,app}$ in the intensity-fraction distributions was not obtained. It is assumed that this negative result reflects a transient association of limited extent which is open in nature. Peaks in the intensity-fraction distributions assignable to micellar associates have been recorded for moderately concentrated solutions of other oxyethylene/oxybutylene block copolymers, i.e. for micellar solutions of mixtures of B_nE_m and $B_nE_mB_n$ copolymers where the latter had relatively lengthy B blocks.[47]

3.8. Effect of Chain Architecture.

3.8.1. $B_nE_mB_n$ and E_mB_n. In Figure 13a, comparison of the present results is made with critical micelle concentrations reported for E_mB_n diblock copolymers with similar E-block lengths in aqueous solution at 30 °C. The logarithm of the cmc is plotted against the total B content, i.e. $x = n$ or $x = 2n$ as appropriate. The necessary data are listed in Table 5. The cmc values of the $B_nE_mB_n$ copolymers at 30 °C were read from Figure 7. The values for the E_mB_n copolymers were taken from a recent compilation,[20] the results listed being copolymers prepared by polymerizing the E-block first. Some scatter derives from the effect of different E-block lengths within the E_mB_n copolymer set, though this effect is small compared to that of the B-block length.[20] It is possible to conclude that the cmc scales exponentially with x, as predicted for a strongly incompatible system.[49,50] The slopes of the lines drawn through the points are: $B_nE_mB_n$, -0.48 ± 0.05; E_mB_n, -0.42 ± 0.05.

Given the experimental error, it is seen that the incremental effect of increasing the number of B-units does not differ greatly between E_mB_n and $B_nE_mB_n$ copolymers. The cmc values of copolymers with a given value of x rank in the order $B_nE_mB_n > E_mB_n$.

By considering, for example, copolymers containing 10 B-units and reading from the lines drawn in Figure 13a, the cmc of a $B_5E_mB_5$ copolymer is about 200 times larger than that of an E_mB_{10} copolymer.

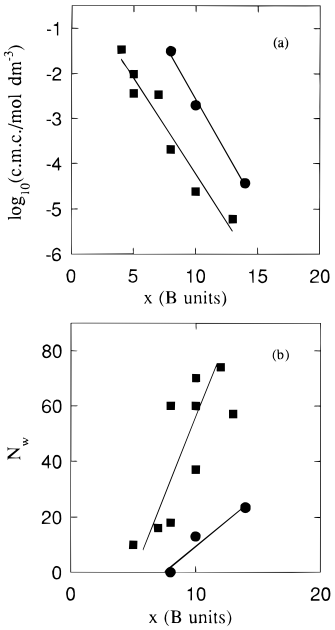

Figure 13. (a) Logarithm of critical micelle concentration (cmc in mol dm^{-3}) *versus* B content (x) for aqueous solutions of triblock ($B_nE_mB_n$) and diblock (E_mB_n) copolymers at 30 °C. (b) Association number (N_w) *versus* B content (x) for aqueous solutions of triblock ($B_nE_mB_n$) and diblock (E_mB_n) copolymers at 30 °C. In both a and b the symbols denote (■) E_mB_n and (●) $B_nE_mB_n$; see Table 5 for details. Note that $x = n$ for copolymers E_mB_n but that $x = 2n$ for copolymers $B_nE_mB_n$.

Table 5. Block Copolymer Micelles: Summary of Data

copolymer	M_n[a] g mol^{-1}	wt % E[a]	−log-(cmc/mol dm^{-3}) at 30 °C	N_w[b] at 30 °C	ref
$E_{50}B_4$	2490	88	1.47		16
$E_{27}B_5$	1550	77	2.01		16
$E_{28}B_5$	1590	75	2.44	10	17
$E_{27}B_7$	1690	70	2.47	16	17
$E_{30}B_8$	1900	70		60	17
$E_{49}B_8$	2730	79	3.69	18	16
$E_{24}B_{10}$	1780	62	4.62	70	16
$E_{32}B_{10}$	2130	66		60	17
$E_{41}B_{10}$	2520	71		37	18
$E_{38}B_{12}$	2540	66		74	20
$E_{50}B_{13}$	3140	70	5.22	57	16
$E_{21}B_8E_{21}$	2420	76	2.60	4	19
$E_{21}B_{11}E_{21}$	2640	70	3.94	25	20
$E_{35}B_{11}E_{35}$[c]	3870	80	3.07		11
$E_{45}B_{14}E_{45}$[c]	4970	80	4.37	10	11,48
$E_{40}B_{15}E_{40}$	4600	77	4.47	15	14
$E_{58}B_{17}E_{58}$	6400	80	4.33	13	12
$E_{71}B_{28}E_{71}$	8260	76		41	13
$B_4E_{40}B_4$	2340	75	1.50		present work
$B_5E_{39}B_5$	2440	70	2.71	14	present work
$B_7E_{40}B_7$	2770	62	4.44[d]	23[d]	present work

[a] Molar masses (M_n) and compositions (wt % E) calculated from formulae given in references. [b] $N_w = M_w$(micelles)/M_w(molecules). Values corrected to 30 °C if necessary. See ref **20** and present text for details. [c] Dow Chemical Co., specified formulae. [d] Values for hypothetical solutions of copolymer $B_7E_{40}B_7$ at 30 °C (i.e. above the cloud point) obtained from values measured at lower temperatures.

Because of the necessary correction procedure, the molar masses obtained for the micelles of the $B_nE_mB_n$ copolymer, and hence their association numbers, carry a high uncertainty, e.g. up to ±20%; see Table 2. However the values listed were stable to sensible variation of the correction parameters and so can be reliably compared with corresponding results obtained for similar copolymers with different block architec-

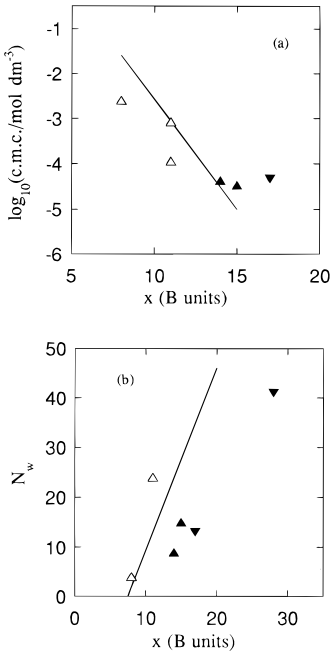

Figure 14. (a) Logarithm of critical micelle concentration (cmc in mol dm^{-3}) *versus* B content (x) for aqueous solutions of triblock ($B_nE_mB_n$ and $E_mB_nE_m$) copolymers at 30 °C. (b) Association number (N_w) *versus* B content (x) for aqueous solutions of triblock ($B_nE_mB_n$ and $E_mB_nE_m$) copolymers at 30 °C. The lines denote the results for the $B_nE_mB_n$. These were taken from Figure 13 and extrapolated as necessary. The triangles denote the results for $E_mB_nE_m$ copolymers and indicate their E-block lengths: (△) $<E_{40}$; (▲) E_{40}-E_{45}; (▼) $>E_{50}$; see Table 5 for details. Note that $x = n$ for copolymers $E_mB_nE_m$ but that $x = 2n$ for copolymers $B_nE_mB_n$.

tures. The temperature dependence of association number N_w is not known for $B_nE_mB_n$ copolymers. However, it is clear from the comparisons made in Figure 8 and previously[19] that, as expected, N_w increases with an increase in temperature. Reported results for micelles of $E_mB_nE_m$ copolymers[12,14,20] indicate an approximately 3% increase in N_w per degree, i.e. $(1/N_w)(dN_w/dT) = 0.03 \pm 0.01$. The values of N_w for $B_nE_mB_n$ copolymer solutions at 30 °C which are plotted in Figure 13b were obtained by adopting this value and also by recognizing that micellization was not detected at 30 °C for copolymer $B_4E_{40}B_4$.[19] The correction (where appropriate) was approximately +1. The association numbers for the E_mB_n copolymers (see Table 5) were taken from ref 20. Within the experimental uncertainty, the association numbers of both types of copolymer can be scaled as the first power of x, though the front factors obviously differ. The ranking order for copolymers of a given x is $E_mB_n > B_nE_mB_n$.

3.8.2. $B_nE_mB_n$ and $E_mB_nE_m$. In considering the available results for $E_mB_nE_m$ copolymers (see Table 5), account was taken of the different reactivities of secondary B and primary E terminal functionalities which leads to a wide E-block length distribution and particularly to the recent conclusion[10] that complete reaction of all terminal groups of B-blocks used to initiate the anionic polymerization of ethylene oxide requires a number-average E-block length of 40 or so B-units. In other words, an $E_mB_nE_m$ copolymer with $m < 40$ contains a proportion of diblock copolymer. This effect does not exist if the E block is polymerized first, as was the case for the other copolymers listed in Table 5. In Figure 14a, copolymers with E-block lengths less than E_{40} are denoted by unfilled symbols, and those with E-block lengths greater or equal to E_{40} by filled symbols. The line represents the results for the $B_nE_mB_n$ copolymers taken from Figure 13a. It is clear that results for the $E_mB_nE_m$ copolymers are affected by their E-block lengths. Considering only the truly triblock copolymers, the ranking order for the cmc values of copolymers with a given value of x is $E_mB_nE_m$ ($m > 40$) ≥ $B_nE_mB_n$.

Association numbers for $E_mB_nE_m$ copolymers (see Table 5, taken from ref 20) are compared with those found for the $B_nE_mB_n$ copolymers in Figure 14b. The line represents the results for the $B_nE_mB_n$ copolymers taken from Figure 13b but extrapolated to higher values of x for convenience of comparison. Again, the effect of E-block length is emphasized by denoting copolymers with E_n on the low and high sides of E_{40} by unfilled and filled symbols, respectively. Considering the true triblock copolymers, the ranking order of N_w for copolymers of a given x is $B_nE_mB_n > E_mB_nE_m$ ($m > 40$).

3.8.3. Comment on Results for E/P Systems. Two direct comparisons have been reported for oxyethylene/oxypropylene copolymers, both based on copolymer L64 (nominally $E_{13}P_{30}E_{13}$), i.e. diblock with triblock ($E_{26}P_{29}$ and $E_{14}P_{30}E_{14}$)[5] and triblock with triblock ($P_{14}E_{24}P_{14}$ and $E_{13}P_{30}E_{13}$).[8] The effect of different reactivities is less pronounced for P end groups than for B end groups, but is important for short E-blocks, such as E_{13}.[10] Accordingly, one would expect differences in critical micelle concentrations and association numbers to be small when comparing with the diblock and large when comparing with the $P_nE_mP_n$ triblock. Reported results confirm this conclusion; e.g. the cmc values and N_w values of $E_{26}P_{29}$ and $E_{14}P_{30}E_{14}$ were found to be almost identical.

3.8.4. Effect of Temperature. In sections 3.7.1 and 3.7.2 critical micelle concentrations and association numbers are compared for different systems at the same temperature. An alternative might be to compare systems at equivalent undercooling from the clouding temperature, i.e. at equivalent values of $T_c - T$. However, for such a comparison to be valid it would be necessary to know the clouding temperatures of molecular solutions, and the present clouding temperatures obtained for 20 g dm^{-3} solutions (section 3.1) are for systems which (at T_c) are predominantly micellar. Phase separation under these circumstances will be into dilute and concentrated micellar phases.[51] The simplest (mean field) models of phase separation of copolymer systems assume identical solubilities for truly molecular solutions of copolymers of identical chain length and overall composition,[52] and if this were the case, comparison of cmc and N_w at a given temperature would be the correct procedure.

3.9. Comparison with Theory. Recently, several authors have addressed the association behavior of triblock copolymers in a poor solvent for the end blocks from a theoretical viewpoint.[24,26,30] The model systems considered differ widely, as explained below, and are not necessarily relevant to the E/B system presently under consideration.

The most closely related study is that of Linse,[24] whose calculations were made for oxyethylene/oxypropylene block copolymers (E_nP_m, $P_nE_mP_n$, $E_mP_nE_m$) of chain length and overall composition equivalent to the commercial copolymer P105 ($E_{37}P_{56}E_{37}$). The ranking orders summarized above for the three E/B systems are close to those predicted by Linse.[24] His values of the cmc and N_w (read from Figures 15 and 16 of ref 24) also show the exponential (cmc) and first power (N_w) dependences found for the E/B copolymers. Quantitative agreement is neither sought nor expected.[24] In fact, the effects of block length are relatively larger in the E/B than in the E/P copolymer systems.

A major concern of Lairez *et al.*[26] was the structure of the associates formed from triblock copolymers in a poor solvent for the end blocks. The system of immediate interest to them was a polystyrene/polyisoprene/polystyrene block copolymer ($S_{550}I_{740}S_{550}$) in heptane, for which they showed that micelles composed exclusively of looped copolymer chains (flower micelles) were less stable than those with a proportion of end blocks extending into the solvent (stripped flower micelles). They concluded, for their system, that the micelles had few looped chains and many extended chains and readily associated to form loose branched structures. The present results for E/B systems are consistent with the initial formation of well-developed micelles, followed by limited micellar association. Of course, different associated structures are expected in systems with widely different chain lengths and interaction energies.[27]

Computer simulations reported by Rodrigues and Mattice[30,31] for triblock copolymers in a poor solvent for the end blocks show an interesting correspondence with our work. In particular, their prediction[30] of transitory (molecular) aggregates, micelles, and bridged micelles provided us with a framework for qualitative interpretation of our light-scattering results. A quantitative (Monte Carlo) study of the problem reported by Nguyen-Misra and Mattice[27] was directed toward rather a different system than the one under discussion here, the relevant results reported being for a series of model copolymers with a short inner block (10 units) and outer blocks from 10 to 25 units each, with parameters chosen to reproduce effects at the weak segregation limit. Not surprisingly, their predicted dependences of the cmc and N_w differ from our experimental findings.

Acknowledgment. We wish to thank Mr. K. Nixon and Dr. F. Heatley, for help in characterizing the copolymers by GPC and NMR, and Prof. S. W. Provencher, who kindly supplied a copy of the CONTIN program. Financial support came from the Government of the Republic of China and the Engineering and Physical Science Research Council.

References and Notes

(1) Wanka, G.; Hoffmann, H.; Ulbricht, W. *Macromolecules* **1994**, *27*, 4145.
(2) Schillen, K; Brown, W.; Johnsen, R. M. *Macromolecules* **1994**, *27*, 4825.
(3) Alexandridis, P.; Holzwarth, J. F.; Hatton, T. A. *Macromolecules* **1994**, *27*, 2414.
(4) Mortenson, K; Pedersen, J. S. *Macromolecules* **1993**, *26*, 805.
(5) Yang, L.; Bedells, A. D.; Attwood D.; Booth, C. *J. Chem. Soc., Faraday Trans.*, **1992**, *88*, 1447.
(6) Yu, G.-E.; Deng, Y.-L.; Dalton, S.; Wang, Q.-G.; Attwood, D.; Price, C.; Booth, C. *J. Chem. Soc., Faraday Trans.* **1992**, *88*, 2537.
(7) Malmsten, M.; Lindman, B. *Macromolecules* **1992**, *25*, 5440.
(8) Zhou, Z.-K.; Chu, B. *Macromolecules* **1994**, *27*, 2025.
(9) Mortensen, K.; Brown, W.; Jorgensen, E. *Macromolecules* **1994**, *27*, 5654.
(10) Nace, V. M.; Whitmarsh, R. H.; Edens, M. W. *J. Am. Oil Chem. Soc.* **1994**, *71*, 777.
(11) Dow Chemical Co., Freeport, Texas, USA, Technical Literature, B-Series Polyglycols. Butylene Oxide/Ethylene Oxide Block Copolymers, 1994.
(12) Luo, Y.-Z.; Nicholas, C. V.; Attwood, D.; Collett, J. H.; Price, C.; Booth, C. *Colloid Polym. Sci.* **1992**, *270*, 1094.
(13) Nicholas, C. V.; Luo, Y.-Z.; Deng, N.-J.; Attwood, D.; Collett, J. H.; Price, C.; Booth, C. *Polymer* **1993**, *34*, 138.
(14) Luo, Y.-Z.; Nicholas, C. V.; Attwood, D.; Collett, J. H.; Price, C.; Booth, C.; Zhou, Z.-K.; Chu, B. *J. Chem. Soc., Faraday Trans.* **1993**, *89*, 539.
(15) Bedells, A. D.; Arafeh, R. M.; Yang, Z.; Attwood, D.; Heatley, F.; Padget, J. C.; Price, C.; Booth, C. *J. Chem. Soc., Faraday Trans.* **1993**, *89*, 1235.
(16) Bedells, A. D.; Arafeh, R. M.; Yang, Z.; Attwood, D.; Padget, J. C.; Price, C.; Booth, C. *J. Chem. Soc., Faraday Trans.* **1993**, *89*, 1243.
(17) Tanodekaew, S.; Deng, N.-J.; Smith, S.; Yang, Y.-W.; Attwood, D., Booth, C. *J. Phys. Chem.* **1993**, *97*, 11847.
(18) Deng, N.-J.; Luo, Y.-Z.; Tanodekaew, S; Bingham, N.; Attwood, D; Booth, C. *J. Polym. Sci., Part A, Polym. Phys.* **1995**, *33*, 1085.
(19) Yang, Z.; Pickard, S.; Deng, N.-J.; Barlow, R. J.; Attwood, D.; Booth, C. *Macromolecules* **1994**, *27*, 2371.
(20) Yang, Y.-W.; Deng, N.-J.; Yu, G.-E.; Zhou, Z.-K.; Attwood, D.; Booth, C. *Langmuir* in press.
(21) Brown, R. A.; Masters, A. J.; Price, C; Yuan, X.-F. In *Comprehensive Polymer Science;* Booth, C., Price, C., Eds.; Pergamon Press: Oxford, 1989; Vol. 2, Chapter 6.
(22) Tuzar, Z.; Kratochvil, P. *Surface and Colloid Science;* Matijevic, E. Ed.; Plenum: New York, 1993; Vol. 15.
(23) ten Brinke, G.; Hadziioannou, G. *Macromolecules* **1987**, *20*, 486.
(24) Linse, P. *Macromolecules* **1993**, *26*, 4437.
(25) Balsara, N. P.; Tirrell, M.; Lodge, T. P. *Macromolecules* **1991**, *24*, 1975
(26) Raspaud, E.; Lairez, D.; Adam, M.; Carton, J.-P. *Macromolecules* **1994**, *27*, 2956.
(27) Nguyen-Misra, M.; Mattice, W. L. *Macromolecules* **1995**, *28*, 1444.
(28) Wang, Y.; Mattice, W. L.; Napper, D. *Macromolecules* **1992**, *25*, 4073.
(29) Alexandridis, P.; Athanassiou, V.; Fukuda, S.; Hatton, T. A. *Langmuir* **1994**, *10*, 2604.
(30) Rodrigues, K.; Mattice, W. L. *Polym. Bull.* **1991**, *25*, 239.
(31) Rodrigues, K.; Mattice, W. L. *Langmuir* **1992**, *8*, 456.
(32) Krauss, S. *J. Phys. Chem.* **1964**, *68*, 1948.
(33) Kotaka, T.; Tanaka, T.; Hattori, M; Inagaki, H. *Macromolecules* **1978**, *11*, 138.
(34) Plestil, J.; Hlavata, D; Hrouz, J; Tuzar, Z. *Polymer* **1990**, *31*, 2112. Tuzar, Z.; Konak, C.; Stepanek, P.; Plestil, J.; Kratochvil, P.; Prochazka, K. *Polymer* **1990**, *31*, 2118.
(35) Knowles, P. R.; Stubbersfield, R. B.; Price, C. *Makromol. Chem., Macromol. Symp.* **1990**, *40*, 203.
(36) Knowles, P. R.; Barlow, R. J.; Heatley, F.; Booth, C.; Price, C. *Macromol. Chem. Phys.* **1994**, *195*, 2547.
(37) Yang, Y.-W.; Zhou, Z.-K.; Barlow, R. J.; Ali-Adib, Z; McKeown, N.; Booth, C., to be published.
(38) Heatley, F.; Yu, G. E.; Sun, W. B.; Pywell, E. J., Mobbs, R. H.; Booth, C. *Eur. Polym. J.* **1990**, *26*, 583.
(39) Provencher, S. W. *Makromol. Chem.* **1979**, *180*, 201.
(40) *Handbook of Chemistry and Physics*, 57th ed.; Weast, R. C., Ed.; CRC Press: Cleveland, 1976; p F-51.
(41) Johnson, B. L.; Smith, J. In *Light Scattering From Polymer Solutions*; Huglin, M. B., Ed.; Academic Press: London, 1972, p 29.
(42) Dixon, A. L.; West, C. J. *International Critical Tables*; McGraw-Hill: New York, 1930; Vol. 7, p 38.
(43) Gulari, E.; Chu, B. *Biopolymers* **1979**, *18*, 2943.
(44) Brown, W.; Johnsen R. M.; Stilbs, P.; Lindman, B. *J. Chem. Phys.* **1983**, *87*, 4548.
(45) Attwood, D.; Collett, J. H.; Tait, C. J. *Int. J. Pharm.* **1985**, *26*, 25.
(46) Vink, H. *J. Chem. Soc., Faraday Trans. 1*, **1985**, *81*, 1725.
(47) Yang, Z.; Yang, Y.-W.; Zhou, Z.-K.; Attwood, D.; Booth, C. *J. Chem. Soc., Faraday Trans.* in press.
(48) Yu, G.-E.; Yang, Y.-W.; Yang, Z.; Attwood, D.; Booth, C.; Nace, V. M. *Langmuir* submitted.
(49) Liebler, L.; Orland, H.; Wheeler, J. C. *J. Chem. Phys.* **1983**, *79*, 3550.
(50) Noolandi, J.; Hong, K. M. *Macromolecules* **1983**, *16*, 1443.
(51) Corti, M.; Minero, C.; Degiorgio, V.; *J. Chem. Phys.* **1984**, *88*, 309.
(52) Flory, P. J. *Principles of Polymer Chemistry* Cornell: Ithaca, NY, 1953.

MA951259I